Quenching weights in DIS
– working notes –

A. Accardi

(Dated: March 22nd, 2007)

I discuss how to use quenching weights in energy loss computations for hadron quenching in nDIS. I also discuss a few ideas on how to implement the computation in the PQM simulation. Finally, I quickly introduce some observables of interest.

I. INTRODUCTION

I will discuss hadron quenching in nuclear Deep Inelastic Scattering (nDIS) in the framework of energy loss models. In particular I will use the Salgado-Wiedemann quenching weights [1] computed in the BDMS formalism. Most formulae come from [2, 3], and several results have been presented in [4].

The nDIS medium, i.e., the target nucleus is very interesting, because it removes 2 of the biggest uncertainties in energy loss computations of hadron quenching in A+A collisions, namely, the initial medium density and its expansion dynamics. Indeed the nuclear density is known and fixed in time. Thus, energy loss models can be tested in nDIS before being applied to A+A collisions.

The kinematic variables are recalled in Fig. 2 and Table I. Note that x, ν, Q^2 are not independent: $x = Q^2/(2M\nu)$ in the target rest frame; in the following I will choose ν and Q^2 as independent variables, because they are the most relevant in our discussion. I would like to remark that in DIS we can experimentally measure all the listed variables, especially ν, Q^2 and z_h. This is markedly different from the situation in hadronic collisions. The hadron energy in nDIS is the analog of p_T in midrapidity hadron production in hadronic collisions. The hadron transverse momentum in DIS, is defined with respect to the photon direction. Its analog in hadronic collisions would be the transverse momentum with respect to the jet axis.

The nuclear geometry is described by the nuclear density distribution $\rho_A(\vec{x})$, where $\vec{x} = (\vec{b}, z)$, z is the coordinate along the direction of the virtual photon and $\vec{b}$ its impact parameter. The center of the nucleus lies at $\vec{x} = (\vec{0}, 0)$. The interaction of the virtual photon γ^* with the quark q happens at $(\vec{b}, y)$. For simplicity, following LO pQCD computations, I assume the quark collinear with the virtual photon, and neglect the parton intrinsic transverse momentum k_T and the hadron mass ($m_h/\nu \to 0$). Then, $E_h \approx z_h \nu$ and the fractional momentum z in the fragmentation functions is $z \approx z_h$, see Appendix A. This assumption should be relaxed when using the PYTHIA generator, primarily because partons are given an intrinsic transverse momentum k_T. The generalized nuclear geometry and the relationship between E_h, z_h, z, ν are discussed in Appendix A.

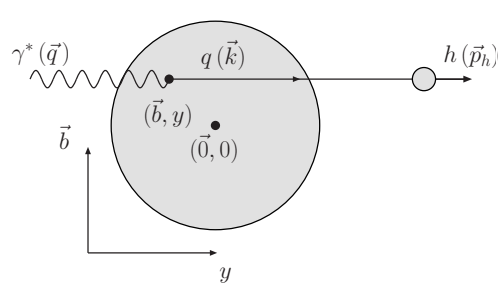

FIG. 1: Geometry of hadron production in nDIS in the nucleus target rest frame. The particles 3-momenta are in parentheses. When the quark is collinear with γ^* the problem is rotationally invariant around the y axis. The non-collinear case is discussed in Appendix A.

I will be interested in calculating the hadron multiplicity ratio R_M defined experimentally as follows:

$$R_M^h(z_h) = \frac{1}{N_A^{DIS}} \frac{dN_A^h(z_h)}{dz_h} \Bigg/ \frac{1}{N_D^{DIS}} \frac{dN_D^h(z_h)}{dz_h}, \qquad (1)$$

i.e., the single hadron multiplicity on a target of mass number A normalized to the multiplicity on a deuteron target as a function of the hadron's fractional energy $z_h = E_h/\nu$, where ν is the virtual photon energy (in the target rest frame). The same ratio can be studied as a function of ν, Q^2 and the hadron transverse momentum p_{hT}.

II. QUENCHING WEIGHTS IN nDIS

A medium is characterized by its transport coefficient, which is defined as the medium-induced transverse momentum squared per unit path length of a probe:

$$\hat{q} = \langle k_T^2 \rangle_{\text{medium}}/\lambda \ , \qquad (2)$$

where λ is the mean free path. For a static and uniform medium of length L, the parameters which characterize medium-induced gluon bremsstrahlung are the characteristic energy ω_c of the radiated gluon, and the size parameter R, which accounts for the fact that the gluon transverse momentum k_T must be smaller than its energy ω:

$$\omega_c = \frac{1}{2}\hat{q}L^2 \qquad (3)$$

$$R = \omega_c L \ . \qquad (4)$$

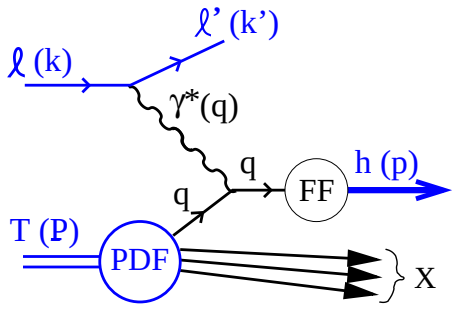

Four-momenta of the particles

Particle	*In target rest frame*
Incident lepton	$k = (E, \vec{k})$
Scattered lepton	$k' = (E', \vec{k'})$
Target nucleon/nucleus	$P = (M, \vec{0})$
Virtual photon	$q = (\nu, \vec{q})$
Produced hadron	$p = (E_h, \vec{p})$

FIG. 2: Semi-inclusive hadron production in deep inelastic scattering on a target T in the pQCD factorization approach at leading order. Parton distribution functions (PDF) and fragmentation functions (FF) represent the non-perturbative input. Four-momenta of the particles involved in the process in the target rest frame are given separately.

Variable	*Covariant*	*Target rest frame*	
Q^2	$= -q^2$	$\simeq 2Mx\nu$	Negative four-momentum squared of the virtual photon.
ν	$= \frac{q\cdot p}{\sqrt{P^2}}$	$= E' - E$	Energy of the virtual photon in the target rest frame.
x	$= \frac{-q^2}{2P\cdot q}$	$= \frac{Q^2}{2M\nu}$	Bjorken scaling variable.
z_h	$= \frac{p\cdot P}{q\cdot P}$	$= \frac{E_h}{\nu}$	Fraction of the virtual photon energy carried by the hadron.
y	$= \frac{q\cdot P}{k\cdot P}$	$= \frac{\nu}{E}$	Fraction of the incident lepton energy transferred to the target.
W^2	$= (P+q)^2$	$= M^2 + 2M\nu - Q^2$	Invariant mass squared of the total hadronic final state.

TABLE I: Definitions of the kinematic variables for semi-inclusive DIS.

The nucleus density is static but non-uniform. We write $\lambda = (\sigma\rho_A)^{-1}$, where σ is the probe cross-section, and assume σ to be fixed and independent of the atomic number. Then, we can define a position-dependent transport coefficient,

$$\hat{q}_A(\vec{b}, y) = \frac{\hat{q}_0}{\rho_0}\rho_A(\vec{b}, y) \ , \tag{5}$$

where $\hat{q}_0 = \hat{q}_{\bar{A}}(0,0)$ is the transport coefficient at the center of a reference nucleus of atomic number $\bar{A}$, and $\rho_0 = \rho_{\bar{A}}(0,0)$.

We consider a quark struck at $(\vec{b}, y)$ which propagates in the nucleus along the y direction. We define its average path-length $\bar{L}_A$:

$$\bar{L}_A(\vec{b}, y) = 2\frac{\int_y^\infty dz\,(z-y)\rho_A(\vec{b}, z)}{\int_y^\infty dz\,\rho_A(\vec{b}, z)} \tag{6}$$

the average nuclear density $\bar{\rho}_A$ seen by the quark:

$$\bar{\rho}_A(\vec{b}, y) = \frac{\int_y^\infty dz\,\rho_A(\vec{b}, z)}{\bar{L}_A(\vec{b}, y)} \ , \tag{7}$$

and, from Eq. (5), the average transport coefficient experienced by the quark:

$$\bar{\hat{q}}_A(\vec{b}, y) = \frac{\hat{q}_0}{\rho_0}\bar{\rho}_A(\vec{b}, y) \ . \tag{8}$$

For a uniform hard-sphere nuclear density $\rho_A(r) = \rho_0\theta(R_A - r)$, the above definitions give $\bar{L}_A = R_A - y$, $\bar{\rho}_A = \rho_0$, and $\bar{\hat{q}}_A = \hat{q}_0$ as it should be.

According to Eqs. (3)-(4), we can define the average characteristic gluon energy $\bar{\omega}_c$ and size parameter $\bar{R}$ as follows:

$$\bar{\omega}_c(\vec{b}, y) \equiv \frac{1}{2}\bar{\hat{q}}_A(\vec{b}, y)\bar{L}_A^2(\vec{b}, y) = \int_y^\infty dz\,(z-y)\hat{q}_A(\vec{b}, z) \tag{9}$$

$$\bar{R}(\vec{b}, y) \equiv \bar{\omega}_c(\vec{b}, y)\bar{L}_A(\vec{b}, y) = \frac{2\bar{\omega}_C^2(\vec{b}, y)}{\int_y^\infty dz\,\hat{q}_A(\vec{b}, z)} \ , \tag{10}$$

where in the last equalities there is no explicit dependence on the definition of the average medium length $\bar{L}_A$. These equations correspond to Eqs. (8) and (10) of Ref. [6]. Note that they depend on only one parameter, $\hat{q}_0$, analog of k in the cited reference. Finally, we can easily see that

$$\bar{\hat{q}}_A(\vec{b}, y) = \frac{2}{\bar{L}_A^2(\vec{b}, y)}\int_y^\infty dz\,(z-y)\hat{q}_A(\vec{b}, z) \ , \tag{11}$$

as in the SW paper [7], see Eq. (7) in Ref. [6]. In that paper it was proven that one can approximate the quenching weight for a dynamically expanding medium with the quenching weight for an equivalent static (and uniform) medium charachterized by the average $\bar{\hat{q}}_A$. However, the natural parameters of the quenching weight are the gluon

charachteristic energy and the size parameter. Hence, the scaling law is more properly expressed by saying that the equivalent static and uniform medium is charachterized by the average $\bar{\omega}_c$ and $\bar{R}$ [6]. In nDIS we have a static but non-uniform medium. For a propagating parton, the spatial non-uniformity is equivalent to a time-evolution of the medium. Therefore, as an *ansatz*, we may generalize the SW scaling law to the case of the static but non-uniform medium encountered in nDIS, and use Eqs. (9)-(10) in the quenching weight evaluation. This *ansatz* will need to be better substantiated in the future.

A few things need to be remarked.

- The SW scaling law has only been established for the special case of a Bjorken-like medium expansion, $\hat{q}(\xi) = \hat{q}_0(\xi_0/\xi)^\alpha$ and $\hat{q}_0 = \hat{q}(\xi_0)$. As remarked above we should remember that in nDIS it is only an *ansatz*.

- The scaling law was shown in [1, 7] to be approximately valid only for $\bar{R} \gtrsim 100$. In applications to nDIS, $\hat{q}_A < 1\text{GeV}^2/\text{fm}$ and one has typically pretty low values of $\bar{R}$ (especially for quark produced close to the far side of the target nucleus and for small nuclei). I did not yet numerically check the typical $\langle \bar{R} \rangle$, but it would be interesting to do.

- $\bar{\omega}_c$ and $\bar{R}$ depend on only 1 parameter, $\hat{q}_0$, which can be fixed on, say, π^+ quenching on a Kr target. An eyeball fit [4] gives $\hat{q}_0 = 0.5 - 0.7$ GeV^2/fm, which is larger than Arleo's fit of $\hat{q} = 0.14$ GeV^2/fm [10, 11]. The reason for this discrepancy, is that Arleo's computation is done at fixed length $\bar{L}_A = (3/4)R_A$, and does not include finite size corrections ($\bar{R} = \infty$). Also, Arleo uses $\alpha_s = 0.5$ and SW use $\alpha_s = 0.3$ in their quenching weight computation. See Sect. VI for a full discussion.

III. ANALYTICAL HADRON QUENCHING COMPUTATION

We assume that the struck quark hadronizes well outside the medium, and that hadron attenuation is due to medium-induced gluon radiation off the quark. At LO, the initial quark energy is $E_q = \nu$. After exiting the medium, the quark energy is reduced to $E_q = \nu - \epsilon$, where ϵ is the total energy of the radiated gluons. This energy loss translates into a modified fragmentation function [4, 11]:

$$\tilde{D}^h_{f/A}(z_h, Q^2; \vec{b}, y) = \int_0^{(1-z_h)\nu} d\epsilon \; p(\epsilon; \bar{\omega}_c, \bar{R}) \times \frac{1}{1-\epsilon/\nu} D^h_f\left(\frac{z_h}{1-\epsilon/\nu}, Q^2\right) + p_0(\bar{R})\, D^h_f(z_h, Q^2) \; , \tag{12}$$

where the dependence on $(\vec{b}, y)$ on the r.h.s. is implicit in $\bar{\omega}_c$ and $\bar{R}$ defined in Eqs. (9)-(10). The quenching weight $\mathcal{P}(\epsilon) = p(\epsilon) + p_0\delta(\epsilon)$ [1] is the probability distribution of an energy loss ϵ, with $p(\epsilon)$ its continuous part and p_0 the probability of no energy loss. The quenching weight is computed for a static and uniform medium with characteristic gluon energy $\bar{\omega}_c$ and size parameter $\bar{R}$. Note that as it stands, (12) implies use of the "non-reweighted" quenching weight of Ref. [6], which amounts to considering absorbed the partons with energy loss $\epsilon \geq E_q$. Use of the "reweighted" quenching weight requires dividing the r.h.s. of (12) by $\int_0^\nu d\epsilon \mathcal{P}(\epsilon)$.

At leading order (LO) in perturbative QCD, the hadron multiplicity is computed as follows:

$$\frac{1}{N_A^{DIS}} \frac{dN_A^h(z_h)}{dz_h} = \frac{1}{\sigma^{lA}} \int_{\text{exp. cuts}} dQ^2\, d\nu \sum_f e_f^2 q_{f/A}(x, Q^2) \times \frac{d\sigma^{lq}}{dQ^2 d\nu} \tilde{D}^h_{f/A}(z_h, Q^2) \; , \tag{13}$$

where we averaged the modified FF according to the distribution of $\gamma^* q$ interaction points:

$$\tilde{D}^h_{f/A}(z_h, Q^2) = \int d^2b\, dy\, \rho_A(\vec{b}, y) \tilde{D}^h_{f/A}(z_h, Q^2; \vec{b}, y) \; . \tag{14}$$

The LO computation is known to underestimate the experimentally measured average $\langle \nu \rangle_{z_h}$ and $\langle Q^2 \rangle_{z_h}$ in each z_h bin [12]. This may result in an incorrect computations of $\tilde{D}^h_{f/A}(z_h, Q^2)$. The problem is likely to be solved at NLO, and is not present in the BUU Monte Carlo simulation of Falter et al. [13]. An effective way of circumventing the problem is to approximate Eq. (13)

$$\frac{1}{N_A^{DIS}} \frac{dN_A^h(z_h, Q^2}{dz_h} \approx \frac{1}{\sigma^{lA}} \sum_f e_f^2 q_f\big(\langle x \rangle_{z_h}, \langle Q^2 \rangle_{z_h}\big) \times \frac{d\sigma^{lq}}{d\langle Q^2 \rangle d\langle \nu \rangle} \tilde{D}^h_{f/A}\big(z_h, \langle Q^2 \rangle_{z_h}\big) \; . \tag{15}$$

The value of the average variables in each z_h-bin is taken from the measured values. Often, $\langle x \rangle$ is not available and is replaced by $\langle x \rangle \approx \langle Q^2 \rangle / (2m_N \langle \nu \rangle)$ [26]

This approach has been used in [4, 5], and a detailed numerical study of pion quenching at HERMES is discussed in Sect. VI.

Remark:

- A criticism of this approach may be found in [8, 9]. I don't quite understand it, though. The "dipole" model presented there also combines induced energy loss (computed in an unconventional way) with prehadron absorption.

IV. IMPLEMENTATION IN PQM

The Parton Quenching Model (PQM) is a Monte Carlo evaluation of the analytical quenching computation in A+A collisions [6]. It is based on PYTHIA to simulate an e+p collision. PYTHIA is based on LO parton cross-section, but due the inclusion of an intrinsic parton momentum it actually generates non-collinear partons. (Some non-collinearity might also be due to the parton generation algorithm; it would be interesting to check this by setting the intrinsic k_T to zero). For this reason, in the following I will not assume $E = \nu$ and $k_T = 0$ as done in the analytic LO pQCD calculations. The generalized fragmentation kinematics is considered in Appendix A.

Here is a possible generalization of the PQM event loop to nDIS. For the definition of experimental cuts, see Appendix D. For definiteness, I assume that the events are stored in suitably defined histograms, but more efficient ways should be considered (as long as they retain information on the variables discussed below).

1. Generate with PYTHIA a quark or gluon satisfying the experimental cuts on x, ν, Q^2, W^2. Extract the ν, Q^2 of the event, and the energy E_k and momentum $\vec{k}$ of the parton. Populate the 6-dimensional DIS event histogram:

$$N(\nu, Q^2, E_k, \vec{k}) \ . \tag{16}$$

   The binning in E_k and $\vec{k}$ is required to study the initial parton spectrum, but is not required if PYTHIA is actually used event-by-event.

2. Sample the $\gamma^* q$ interaction point according to $\rho_A(\vec{b}, y)$; determine $\bar{\omega}_c$ and $\bar{R}$, see Eqs. (A1)-(A2).

3. Sample the energy loss ϵ from $\mathcal{P}(\epsilon)$. If reweighting is desired, sample until $\epsilon < E$.

4. Fragment the parton according to the vacuum $D(z)$, and compute the hadron energy $E_h = E_h(z, E_k, \vec{k})$ from Eq. (A9) and $z_h = E_h/\nu$. Reject the event if it does not satisfy the cuts on z_h and E_h. Populate the 4-dimensional semi-inclusive histogram

$$N^h(\nu, Q^2, z_h, p_{hT}) \tag{17}$$

   It is also interesting to populate

$$\bar{\omega}_c(\nu, Q^2, z_h, p_{hT}); \ \bar{R}(\nu, Q^2, z_h, p_{hT}) \tag{18}$$

$$b(\nu, Q^2, z_h, p_{hT}); \ y(\nu, Q^2, z_h, p_{hT}) \tag{19}$$

$$\zeta(\nu, Q^2, z_h, p_{hT}) \tag{20}$$

   where $\zeta = \epsilon/E$.

5. Go to point 1 until enough DIS events or semi-inclusive events have been generated.

To save time, it is also possible to precompute the spectrum $N(\nu, Q^2, E_k, \vec{k})$. In this case, the binning in E_k and $\vec{k}$ is necessary. Then point 1 above can be replaced by

1b. Use the precomputed $N(\nu, Q^2, E_k, \vec{k})$ to sample the event's ν and Q^2, and the parton energy and momentum, E and $\vec{k}$.

The 2 methods are equivalent. The second might be preferred to save time when considering several nuclei, or several transport coefficients. Care should be taken to avoid systematic effects, as for example in the case of a limited number of simulated events. Note that unless the non-collinearity of the parton and photon turns out to be irrelevant, it is difficult to interpolate the spectrum for smoothness. It is preferrable to run PYTHIA long enough to achieve the desired accuracy in the histograms, provided enough computer time is available.

V. OBSERVABLES

Given the histograms defined in the previous section, we may build many observables. As a concrete example, I will concentrate on z_h distributions, and discuss interesting quantities to be studied. Analogously, one can discuss ν- or Q^2-distributions, or go for a multi-variable analysis.

An important check is the degree of non-collinearity of the photon and the struck parton, and the real need for the generalized fragmentation kinematics of Appendix A. For example, we may study the relationship between E and ν as a scatter plot in the ν, E_k plane using

$$N^{\nu E}(\nu, E_k) = \sum_{j,n} N(\nu, Q_j^2, E_k, \vec{k}_n) \tag{21}$$

or plotting the average $\langle E \rangle$ as a function of ν:

$$\langle E_k(\nu) \rangle = \frac{\sum_{i,j,n} E_{k|j} N(\nu, Q_i^2, E_{k|j}, \vec{k}_n)}{\sum_{i,j,n} \bar{N}(\nu, Q_i^2, E_{k|j}, \vec{k}_n)} \ . \tag{22}$$

(Note the compact notation: $\vec{k}_n$ actually are 3 different variables.) A complementary study can be done by computing $\langle \vec{k}^2 \rangle^{1/2}$. Alternatively, we can compute $\langle \theta \rangle$ where theta is the angle $\theta = \arctan(|k_T|/k_z)$ (which would need some extra binning of N at point 1 in the PQM loop).

Next, let's consider the experimental observables. The number of DIS events, independently of the parton's energy, is

$$N^{DIS}(\nu, Q^2) = \sum_{m,n} N(\nu, Q^2, E_{k|m}, \vec{k}_n) \ . \tag{23}$$

The hadron z_h-spectrum is defined as

$$\frac{1}{N_A^{DIS}} \frac{dN_A^h}{dz_h} = \frac{1}{\Delta z \sum_{i,j} N^{DIS}(\nu_i, Q_j^2)} \times \sum_{i,j,l} N^h(\nu_i, Q_j^2, z_h, p_{hT|l}) \ , \tag{24}$$

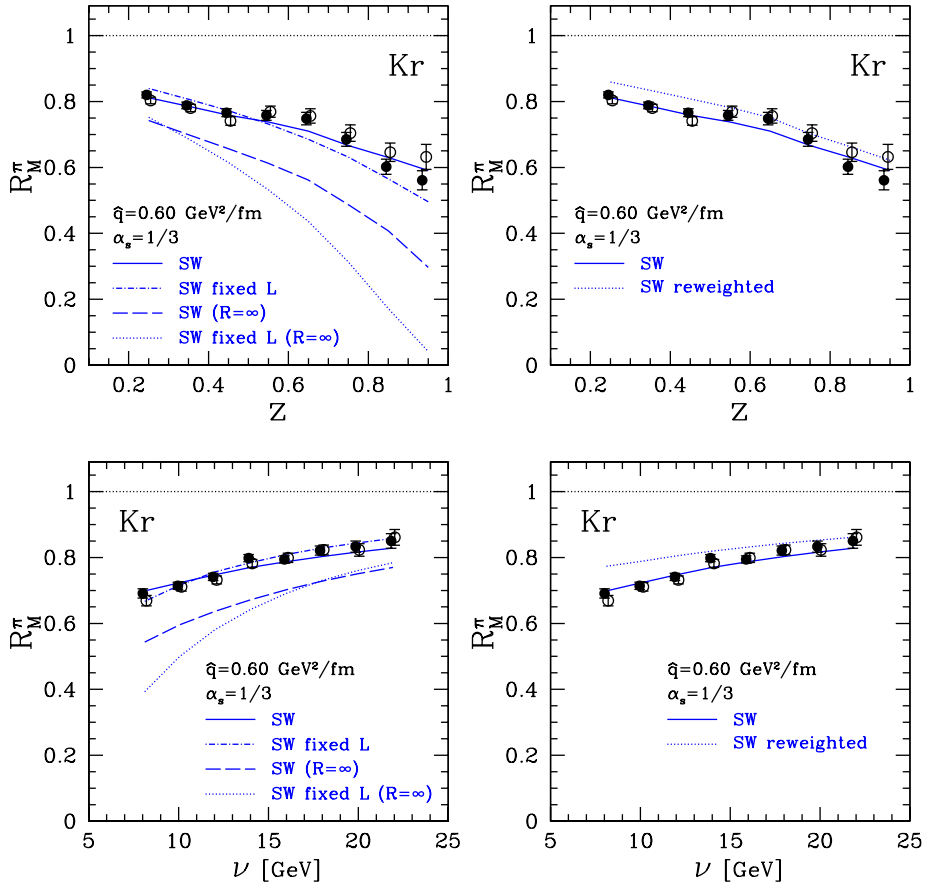

FIG. 3: Pion quenching on Krypton target calculated with SW quenching weights. Left: realistic and approximate treatments of the nuclear geometry. Right: effect of energy conservation corrections. The lines are described in the text. Experimental data are from the HERMES collaboration [17]. Full symbols for π^+ and open simbols for π^- have been slighlty shifted to the left and right for better display.

from which the attenuation ratio $R_M(z_h)$ can be constructed. The average $\langle\nu\rangle_{z_h}$, and similarly $\langle Q^2\rangle_{z_h}$, is

$$\langle\nu\rangle_{z_h} = \frac{\sum_{i,j,l}\nu_i N^h(\nu_i, Q_j^2, z_h, p_{hT|l})}{\sum_{i,j,l} N^h(\nu_i, Q_j^2, z_h, p_{hT|l})} \ . \qquad (25)$$

It is then interesting to check the obtained average kinematic variables values against experimental data.

The energy loss process may be characterized by the average $\langle\bar{R}\rangle_{z_h}$, $\langle\bar{\omega}_c\rangle_{z_h}$, and $\langle\zeta\rangle_{z_h}$. They are defined, e.g., as

$$\langle\bar{R}\rangle_{z_h} = \frac{\sum_{i,j,l}\bar{R}(\nu_i, Q_j^2, z_h, p_{hT|l})}{\sum_{i,j,l} N^h(\nu_i, Q_j^2, z_h, p_{hT|l})} \ . \qquad (26)$$

$\langle\bar{R}\rangle$ will give an idea of the strength of the finite size corrections applied; $\langle\zeta\rangle = \langle\epsilon/E\rangle$ gives an estimate for the need of reweighting [6] or $1/\nu$ corrections [14].

Other quantities of interest:

- distribution of $\gamma^* q$ interaction points in single-inclusive hadron production.
- Quenching of different flavors – at HERMES they measure charge-separated π, K, p.
- Cronin effect: with energy loss and/or Fermi motion effects (see Appendix C for further details).
- Quenching at various experiments:
  1. EMC – $E_{lab} = 100$ and 200 GeV
  2. HERMES – $E_{lab} = 27.5$ and 12 GeV
  3. JLAB – $E_{lab} = 12$ and 6 GeV

The study of dihadron attenuation [15] is also very interesting because up to now no model gets it right: neither hadron absorption nor energy loss. However it would probably require more effort, because at LO only 1 hadron is generated in the interaction, and the KKP fragmentation function are for single hadrons only. A possibility is to directly use the JETSET module of PYTHIA instead of KKP to fragment the produced partons. However, one should go a bit inside PYTHIA to subtract the energy loss from the parton before fragmenting it. So,

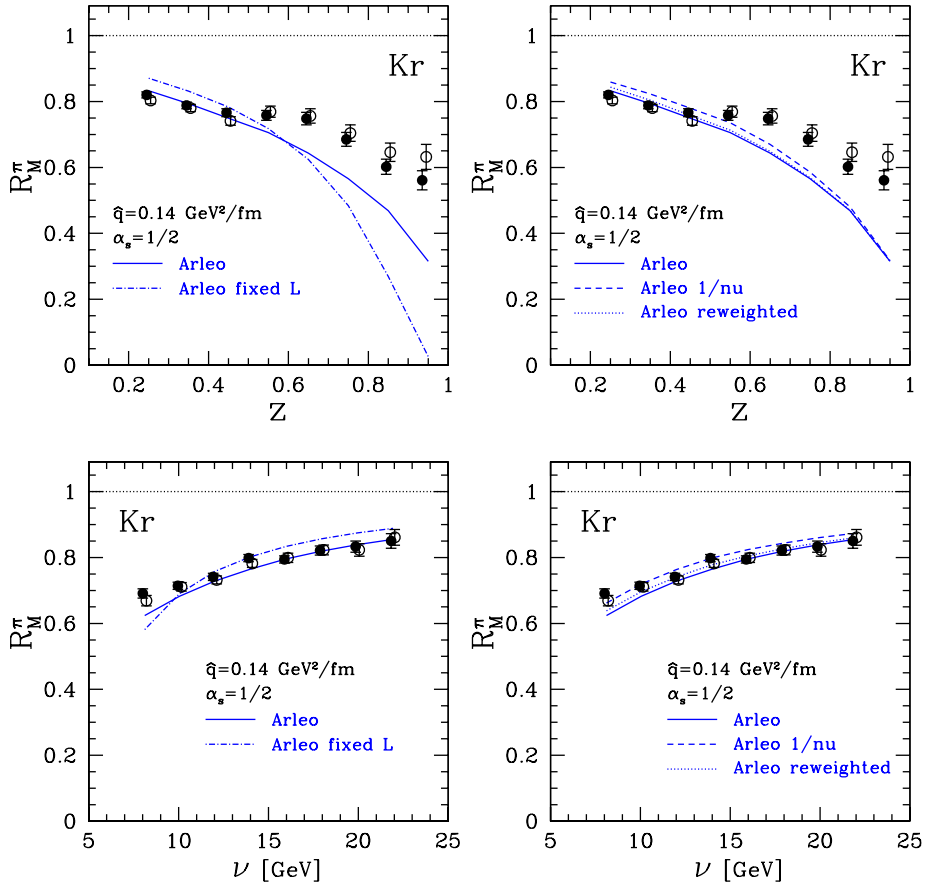

FIG. 4: As Fig. 3 but calculated with Arleo's quenching weights (only the $R\to\infty$ case is available).

I would suggest to leave it for eventual future developments.

Any other idea is welcome!

VI. ANALYTIC QUENCHING RESULTS

I report here a study of $\pi^\pm$ quenching at HERMES in the analytic quenching model of Sect. III. The computations have been done by further approximating Eq. (15) as an isospin averaged sum of up and down quark fragmentation functions:

$$\frac{dN_A^{\pi^\pm}(z_h,Q^2)}{dz_h} \approx \left\langle D_u^{\pi^\pm}\left(z_h,\langle Q^2\rangle_{z_h}\right) + D_d^{\pi^\pm}\left(z_h,\langle Q^2\rangle_{z_h}\right)\right\rangle_{A,Z} \tag{27}$$

This approximation is a bit rough, as it does not take into account the right mix of quarks and anti-quarks (plus it neglects strange quarks altogether). However, it fairly reproduces the computation in Arleo's paper [11] with a tendency to overshoot it. So, I consider Eq. (27) a fair approximation to a full computation. Finally, I plot

$$R_M^h \approx dN_A^h/dN_D^h \ . \tag{28}$$

The results are shown in Figs. 3 and 4 using, viz., SW quenching weights with $\alpha_s = 1/3$ [1] and Arleo's quenching weights with $\alpha_s = 1/2$ [14]. Note that Arleo's quenching weights are computed only in the asymptotic medium limit $R\to\infty$. I determined the quenching weight by an eyeball fit of the "full-geometry" computation represented by the solid lines. The result is $\hat{q}_0 = 0.5 - 0.7$ GeV^2/fm and $\hat{q}_0 \approx 0.15 - 0.20$ GeV^2/fm, respectively. The difference is due to a) the difference in the α_s used [27], and most importantly b) the use of finite R in one case and $R\to\infty$ in the other (see also the discussion below).

I will discuss 2 important aspects of these computations: the importance of correctly account for the medium geometry [4], and the effect of energy conservation corrections to insure that $\epsilon \le E$.

Let's start with nuclear geometry. The relevant plot are the left ones in the figures. The crudest approximation is to use an average quark path-length $L \approx (4/3)R_A$, asymptotic quenching weights ($R\to\infty$) and a constant nuclear density, corresponding to a constant transport coefficient $\hat{q}$ (dotted line). This approximation is commonly considered, but as we can see it cannot at all reproduce the slope of the data, and would require a much

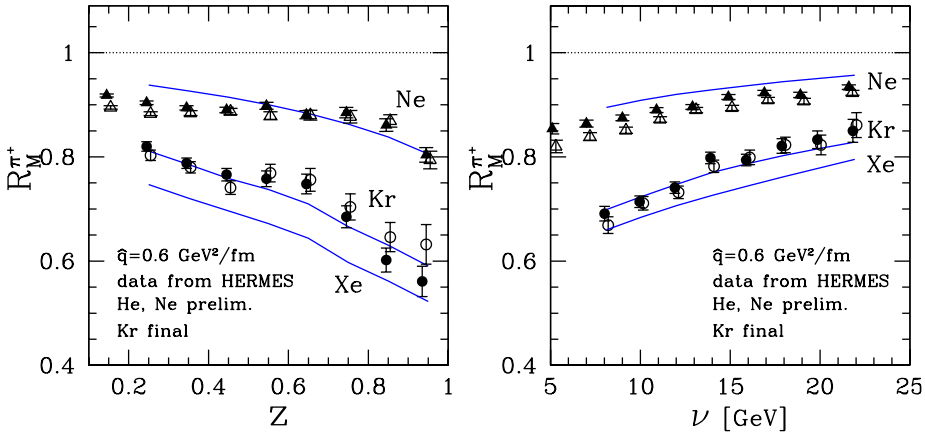

FIG. 5: Pion quenching for different nuclei compared to full-geometry, non reweighted SW computations. Experimental data are from the HERMES collaboration [17, 18]. Full symbols for π^+ and open simbols for π^- have been slighlty shifted to the left and right for better display.

smaller $\hat{q} \approx 0.2$ GeV^2/fm to touch the data. We can relax these approximations in several steps: using asymptotic quenching weights with a variable medium length (dashed line), non-asymptotic quenching weights (finite $R = \omega_c L$ with fixed average L (dot-dashed line) and with variable L (solid line). The biggest effect is given by the use of non-asymptotic quenching weights. Use of variable versus average length gives a smaller but still important effect. As already remarked, the extraction of the quenching parameter from the data strongly depends on the approximation used.

The effect of energy conservation is shown in the right plots in each figure. The constraint $\epsilon \leq E_q$ can be imposed by cutting the quenching weight at $\epsilon = E_q$ and reweighting it to conserve probability [6]. Alternatively, on can cut the single gluon radiation spectrum at $\omega = E$, and consider $O(\omega_c/E_q)$ corrections [14]; the energy lost through multiple gluon radiation can still be larger than E, but the problem becomes much less severe, as we will see. The energy conservation corrections tend to reduce the quenching for a given $\hat{q}_0$. Their effect increases with $\hat{q}_0$ and A, and decreases with z_h. The magnitude is about 5-10% for Kr targets, and typically comparable to the experimental error bars in the figure. Thus they are subleading compared to the effect of correctly implementing the nuclear geometry. It's interesting to note that the $O(\omega_c/E_q)$ corrections are larger than the reweighting correction, at least in the explored range of $\hat{q}$. Further reweighting the $O(\omega_c/E_q)$-corrected spectrum has almost no effect, and the corresponding computation is not shown in the plots. This shows that after accounting $O(\omega_c/E_q)$, the probability of radiating an energy $\omega > E$ becomes negligible. For larger values of $\hat{q}_0$, as found in A+A collisions, this might not be anymor true.

Finally, in Fig. 5 I compare the full-geometry, non reweighted SW computation to the A-dependence of the experimental quenching. The model can reasonably describe quenching for medium-heavy nuclei at $z_h \gtrsim 0.4$. When comparing the theoretical ν-distribution with data, keep in mind that $\langle z_h \rangle_\nu \approx 0.3$, where the model tends to overestimate the data (see left panel). For ^{4}He target, I don't trust much the model to start with. In fact, ^{4}He is a pretty compact and small object, for which the approximate treatment of nuclear effects which I employed might be insufficient.

APPENDIX A: NUCLEAR GEOMETRY AND FRAGMENTATION KINEMATICS

If we relax the LO assumption that the quark is collinear with the virtual photon (Fig. 6), the definitions

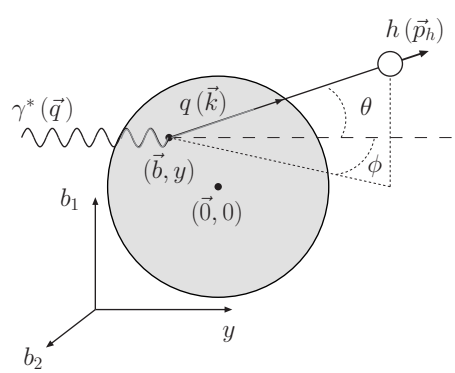

FIG. 6: Geometry of hadron production in nDIS in the nucleus target rest frame with non collinear quark and virtual photon. The particles 3-momenta are in parentheses. Note that $\vec{k}$ does not lie in the (b_1, y) plane as $\vec{q}$ does.

of $\bar{\omega}_c$ and $\bar{R}$ in Eqs. (9)-(10) should read:

$$\bar{\omega}_c(\vec{b}, y) = \int_0^\infty d\xi\, \xi\, \hat{q}_A(\vec{x}_0 + \xi\vec{n}) \tag{A1}$$

$$\bar{R}(\vec{b}, y) = \frac{2\bar{\omega}_C^2(b, y)}{\int_0^\infty d\xi\, \hat{q}_A(\vec{x}_0 + \xi\vec{n})} \ , \tag{A2}$$

where $\vec{x}_0 = (\vec{b}, y)$ and $\vec{n} = \vec{k}/|\vec{k}|$, and $\vec{k}$ is the 3-momentum of the quark. The degree of non collinearity may be quantified by the quark angle relative to the photon

$$\theta = \arctan \frac{|\vec{k}_T|}{k_z} \ . \tag{A3}$$

However, note that θ alone does not charachterize the direction of motion of the quark, which would also require the angle ϕ in Fig. 6.

For fragmentation, some care is needed, because the z entering the FF is defined as $z = p_h^+/p_q^+$ (with light-cone plus-momentum $p^+ = (E + p_z)/\sqrt{2}$, see Appendix B), whereas the DIS invariant is $z_h = p{\cdot}P/q{\cdot}P = E_h/\nu$ in the target rest frame. Therefore, the equations $E_h = zE_q$, $z_h = z$ used in Sect. III are only valid in a special limiting case, as we will see. The 4-momenta k of the parton in light-cone and normal coordinates is, respectively,

$$k^\mu = (k^+, \frac{k_T^2}{2k^+}, \vec{k}_T) = (E_k, \vec{k}_T, \sqrt{E_k^2 - k_T^2}) \ , \tag{A4}$$

where the k^- (k_3) component has been fixed so that $k^2 = 0$ (putting the parton on-shell **might be wrong, I am not sure**). The generalization to a massive quark is trivial. The 4-momentum of the produced hadron is p_h. **If I understand well**, by definition of the fragmentation variable z, we have [20]

$$p_h^+ = zk^+ \tag{A5}$$

$$\vec{p}_{hT} = z\vec{k}_T \ . \tag{A6}$$

Note that this is different from Refs. [21, 22], which define $z = E_h/E_k$. Since the hadron is on-shell with mass m_h, we obtain

$$p_h = (zk^+, \frac{m_{hT}^2}{2zk^+}, z\vec{k}_T) = (E_h, z\vec{k_T}, \sqrt{E_h^2 - m_{hT}^2}) \ , \tag{A7}$$

where

$$m_{hT}^2 = m_h^2 + (zk_T)^2 \ . \tag{A8}$$

Next, we want to express the invariant z_h as a function of z. Using the definition of z in (A5), we have:

$$z = \frac{E_h + \sqrt{E_h^2 - m_{hT}^2}}{E_k + \sqrt{E_k^2 - k_T^2}}$$

Inverting it, we can find E_h (and $z_h = E_h/\nu$) as a function of z,

$$E_h = zE_k \frac{1 + \sqrt{1 - k_T^2/E_k^2}}{2} \times \left[1 - \left(\frac{m_{hT}}{zE_k(1 - \sqrt{1 + k_T^2/E_k^2}}\right)^2\right] \tag{A9}$$

This is the most general expression for E_h. It is very suitable for implementation in PQM, because the 3-momentum of the parton is known from PYTHIA, and z from the sampling of $D(z)$.

We can study some special cases. In the limit of large parton energy, $m_{hT}/E_k{\to}0$ and $k_T/E_k{\to}0$, we obtain

$$E_h \xrightarrow[\text{large } E_k]{} zE_k \ . \tag{A10}$$

We can also consider the "LO approximation": we assume the parton to have no intrinsic momentum, so that $k \approx (\nu, \vec{0}_T, \nu)$ by momentum conservation (see Fig. 2). From (A9), we obtain

$$E_h \xrightarrow[LO]{} z\nu \left[1 - \left(\frac{m_h}{2z\nu}\right)^2\right] \ . \tag{A11}$$

If we further assume a large parton energy, $m_h/\nu{\to}0$, we obtain

$$E_h \xrightarrow[\text{large } \nu]{} z\nu \ , \tag{A12}$$

which parallels Eq. (A10) and explains the approximation $z \approx z_h$ used in the analytic computations of Sect. III.

In nDIS at HERMES, $E_h \approx z_h\nu = 2 - 20$ GeV, so that the limit of large quark energy, Eq. (A10) [or Eq. (A12)] might not be justified at low z_h or low ν. Using the full Eq. (A9) [or Eq. (A11)] is probably needed for hadrons heavier than pions, and definitely important for heavy flavors like D mesons.

Note that since E_h must be positive, Eq. (A9) imposes a lower bound on z:

$$z \geq \frac{m_{hT}}{E_k}\left(1 + \sqrt{1 - k_T^2/E_k^2}\right) \xrightarrow[LO]{} 2\frac{m_h}{\nu} \ . \tag{A13}$$

This bound needs not be implemented in PQM as long as the experimental cuts require $E_h > E_{h,min}$ with $E_{h,min} > 2m_h$, which is typically the case. In analytic computations it is of concern only if $2m_h/\nu$ exceeds the experimental $z_{h|min}$.

The next step is to implement energy loss. In the PQM philosophy, we generate a parton with a given E_k, which loses an amount ϵ of energy according to the quenching weight $\mathcal{P}(\epsilon)$. The parton energy and momentum prior to hadronization are

$$E_k' = E_k(1 - \epsilon/E_k)$$
$$\vec{k'} = \vec{k}(1 - \epsilon/E_k) \ . \tag{A14}$$

Then, the hadron energy is simply given by Eq. (A9) with $E_k \to E'_k$ and $\vec{k}_T \to \vec{k'}_T$. In the high-ν LO approximation, we obtain $E_h = z(\nu - \epsilon)$ as used in the main text.

Note that Eq. (A14) is only valid for a massless quark. For massive quarks, we need to define k'_3 such that $k'^2 = M_q^2$. **I will consider this generalization in the near future.**

APPENDIX B: LIGHT-CONE COORDINATES

The light-cone plus- and minus- momenta are defined for any 4-vector $a_\mu = (E_a, a_1, a_2, a_3) = (E_a, \vec{a}_T, a_3)$ by

$$a^\pm = \frac{1}{\sqrt{2}}(E_a \pm a_3) \ , \tag{B1}$$

and conversely

$$\begin{aligned} E_a &= \frac{1}{\sqrt{2}}(a^+ + a^-) \\ a_3 &= \frac{1}{\sqrt{2}}(a^+ - a^-) \ . \end{aligned} \tag{B2}$$

In light-cone coordinates, we represent a as

$$a = (a^+, a^-, \vec{a}_T) \ . \tag{B3}$$

The dot-product is

$$a \cdot b = a^+ b^- + a^- b^+ - \vec{a}_T \cdot \vec{b}_T \ . \tag{B4}$$

In nDIS, the reference frame is defined by the momentum q of the virtual photon and p of the target:

$$\begin{aligned} p^\mu &= p^+ \overline{n}^\mu + \frac{m^2}{2p^+} n^\mu \\ q^\mu &= -x_B p^+ \overline{n}^\mu + \frac{Q^2}{2x_B p^+} n^\mu \end{aligned} \tag{B5}$$

where p^+ is a boost parameter, and $\overline{n} = (1/\sqrt{2}, \vec{0}_\perp, 1/\sqrt{2})$, $n = (1/\sqrt{2}, \vec{0}_\perp, -1/\sqrt{2})$ define the "plus" and "minus" light-cone directions. In the target rest frame ($p^+ = M/\sqrt{2}$) the 2 momenta read:

$$\begin{aligned} p &= \Big(\frac{M}{\sqrt{2}}, \frac{M}{\sqrt{2}}, \vec{0}_T\Big) \\ q &= \Big(\frac{x_B M}{\sqrt{2}}, \frac{Q^2}{\sqrt{2} x_B M}, \vec{0}_T\Big) \end{aligned} \tag{B6}$$

APPENDIX C: CRONIN EFFECT

The Cronin effect is the nuclear modification of the hadron p_{hT} spectrum, where p_{hT} is defined relative to the photon axis. In nDIS one defines a "Cronin ratio" as

$$R_M^h(p_{hT}) = \frac{1}{N_A^{DIS}} \frac{dN_A^h(p_{hT})}{dp_{hT}} \Bigg/ \frac{1}{N_D^{DIS}} \frac{dN_D^h(p_{hT})}{dp_{hT}} \ . \tag{C1}$$

Experimentally, one observes a suppression of R_M below 1 at low $p_{hT} \lesssim 1$ GeV, and a rapid increase of R_M above 1 at larger hadron transverse momenta. I will discuss 2 possible mechanisms for the Cronin effect: the medium-induced parton momentum broadening, and the nucleon Fermi motion.

In the BDMPS energy loss framework, the transverse momentum kick that a static and uniform medium transfers to the parton is related to the transport coefficient [23, 24]:

$$\langle m_T^2 \rangle = \frac{C_R}{C_A} \hat{q} L \ , \tag{C2}$$

where $\vec{m}_T$ is the transverse momentum gained by the parton relative to its initial direction of motion $\vec{k}$. However, this equation holds only in the $L/\lambda \to \infty$ limit. Using our *ansatz* of replacing $\hat{q} \to q$ and $L \to \bar{L}_A$, we obtain, in the collinear quark approximation:

$$\langle m_T^2 \rangle = \frac{C_R}{C_A} \bar{\hat{q}}(\vec{b}, y) \bar{L}_A(\vec{b}, y) = \frac{C_R}{C_A} \int_y^\infty dz \, \hat{q}_A(\vec{b}, z) \tag{C3}$$

which on the r.h.s. does not explicitly depend on $\bar{L}_A$. Perhaps, a more sound starting point for non-asymptotic media is to use relationship between $\langle m_T^2 \rangle$ and $\langle \epsilon \rangle$

$$\langle m_T^2 \rangle = \frac{8}{\alpha_s N_c} \frac{\langle \epsilon \rangle}{L} \ , \tag{C4}$$

which is valid also for finite-length matter, cold or hot, and is independent of the parton nature [23]. In this case, one uses the scaling law to compute

$$\langle \epsilon \rangle = \int d\epsilon \, \epsilon \, \mathcal{P}(\epsilon, \bar{\omega}_c, \bar{R}) \ , \tag{C5}$$

and replaces $L \to \bar{L}_A$ in (C4). The dependence on $\bar{L}_A$ is not fully cancelled, because $\langle \epsilon \rangle \propto \bar{\hat{q}} \bar{L}_A^2 \propto \bar{L}_A$ is only valid asymptotically. Thus, we might have a divergence of $\langle m_T^2 \rangle$ as $\bar{L}_A \to 0$ if $\langle \epsilon \rangle$ is less than linear in $\bar{L}_A$ in that limit (**we should check this point.**) To take into account fluctuations in the momentum broadening, we may assume a Gaussian distribution for its modulus $m_T = |\vec{m}_T|$

$$\mathcal{G}(m_T) = \frac{1}{\sqrt{2\pi \langle m_T^2 \rangle}} \exp(-m_T^2/(2\langle m_T^2 \rangle) \ , \tag{C6}$$

with $\vec{m}_T$ uniformly distributed around the parton momentum $\vec{k}$ [28]. We should remark that the Gaussian approximation is correct in the limit of large broadening (a consequence of the central limit theorem), which is not necessarily realized in nDIS with small $\hat{q}$. The final quark momentum before fragmentation should read:

$$\vec{k}' = (1 - \zeta)\vec{k} + \vec{m}_T \ , \tag{C7}$$

where ζ is the fractional energy loss. Since the parton broadening increases with A the broadening induces a Cronin effect. Note that energy-loss has 2 effects: one

is to broaden the parton momentum, which induces a Cronin enhancement at large parton momenta; the other is to quench the parton spectrum prior to hadronization, which gives a Cronin suppression at all momenta. The 2 effects compete, so it is difficult to predict the net effect on the Cronin ratio $R_M(p_T)$.

The second mechanism is nucleon Fermi motion. The nucleon momentum distribution $n(\vec{l})$ in the target rest rest frame can be computed, e.g., in non-relativistic models of the nuclear structure. Then we should modify the initial momentum of the quark according to

$$\vec{k} \to \vec{k} + \vec{l}\,. \tag{C8}$$

This prescription may be oversimplified; I will check that it is a reasonable approximation. Since $\langle l^2 \rangle$ is an increasing function of A, Fermi motion induces a Cronin effect. The typical magnitude of the Fermi momentum is $\sqrt{\langle l^2 \rangle} \approx 200 MeV$. Hence the Fermi motion induced Cronin effect might be small in absolute value, and negligible compared to the effect of the momentum transfer from the traversed medium.

APPENDIX D: EXPERIMENTAL CUTS

In Table II, the experimental kinematic cuts are collected. They are divided in DIS cuts ($e + A \to e + X$) and semi-inclusive cuts ($e + A \to e + h + X$). An example of the allowed phase space is presented in Fig. 7.

[1] C. A. Salgado and U. A. Wiedemann, Phys. Rev. D **68** (2003) 014008 [arXiv:hep-ph/0302184].
[2] A. Accardi, notes in the blue INFN notebook, July 2004
[3] A. Accardi, talk at "From RHIC to LHC: achievements and opportunities", INT, Seattle 17 October 2006 [available at http://nt3.phys.columbia.edu/people/aaccardi/talks/].
[4] A. Accardi, Acta Phys. Hung. A **27** (2006) 189.
[5] A. Accardi, Eur. Phys. J. C **49** (2007) 347.
[6] A. Dainese, C. Loizides and G. Paic, Eur. Phys. J. C **38** (2005) 461.
[7] C. A. Salgado and U. A. Wiedemann, Phys. Rev. Lett. **89** (2002) 092303.
[8] B. Z. Kopeliovich, J. Nemchik and I. Schmidt, Nucl. Phys. A **782** (2007) 224 [arXiv:hep-ph/0608044].
[9] B. Z. Kopeliovich, J. Nemchik, E. Predazzi and A. Hayashigaki, Nucl. Phys. A **740** (2004) 211 [arXiv:hep-ph/0311220].
[10] F. Arleo, Phys. Lett. B **532** (2002) 231 [arXiv:hep-ph/0201066].
[11] F. Arleo, Eur. Phys. J. C **30** (2003) 213.
[12] A. Accardi, V. Muccifora and H. J. Pirner, Nucl. Phys. A **720** (2003) 131
[13] T. Falter, W. Cassing, K. Gallmeister and U. Mosel, Phys. Rev. C **70** (2004) 054609.
[14] F. Arleo, JHEP **0211** (2002) 044.
[15] A. Airapetian *et al.* [HERMES], Phys. Rev. Lett. **96** (2006) 162301.
[16] A. Airapetian *et al.* [HERMES Collaboration], Eur. Phys. J. C **21** (2001) 599 [arXiv:hep-ex/0104004].
[17] A. Airapetian *et al.* [HERMES], Phys. Lett. B **577** (2003) 37.
[18] G. Elbakian *et al* [HERMES], Proceedings of "DIS 2003", St.Petersburg, April 23-27, 2003; V.T. Kim and L.N. Lipatov eds., page 597.
[19] P. B. van der Nat [HERMES], http://www-hermes.desy.de/notes/pub/trans-public-subject.html
[20] J. C. Collins and D. E. Soper, Nucl. Phys. B **193** (1981) 381 [Erratum-ibid. B **213** (1983) 545].
[21] K. J. Eskola, H. Honkanen, C. A. Salgado and U. A. Wiedemann, Nucl. Phys. A **747** (2005) 511.
[22] K. J. Eskola and H. Honkanen, Nucl. Phys. A **713** (2003) 167.
[23] R. Baier, Y. L. Dokshitzer, A. H. Mueller, S. Peigne and D. Schiff, Nucl. Phys. B **484** (1997) 265 [arXiv:hep-ph/9608322].
[24] F. Arleo, "Estimates for cold nuclear matter transport coefficients", in Ref. [25], page 141
[25] A. Accardi *et al.*, "Hard probes in heavy ion collisions at the LHC: Jet physics," working group report for CERN Yellow Report, arXiv:hep-ph/0310274.
[26] A numerical check of the difference between Eqs. (13) and (15) is desirable, but I would need to generalize quite a bit my code to perform it.
[27] With $\alpha_s = 1/3$ in Arleo's quenching weights one would roughly obtain $\hat{q}_{1/3} \approx (3/2)\hat{q}_{1/2} = 0.3$ GeV^2/fm. This comes from the fact the $\langle \epsilon \rangle \propto \alpha_s \hat{q}$.
[28] Another way of taking fluctuations into account, would be to use Eq. (C4) directly for m_T^2 and ϵ. This would account for fluctuations arising from multiple gluon emission, but not for fluctuations in the m_T in each gluon radiation process. However, I am not sure how theoretically sound such an ansatz is.

		EMC		HERMES27 N,Kr [17]			HERMES27 He,Ne,Xe [18]			HERMES12 N,Kr [19]	
		h		h	π, K	p	π	K	p	h	π
$E_{\rm beam}$	GeV	100	200	27.5	...	...	27.5	...	...	12	...
$Q^2_{\rm min}$	GeV^2	2	...	1	...	...	1	...	...	0.5	...
$W^2_{\rm min}$	GeV^2	4	...	4	...	...	4	...	...	4	...
$x_{\rm min}$		0.02	...	0.02	...	...	0.02	...	...	0.01	...
$x_{\rm max}$		1	...	1	...	...	1	...	...	1	...
$\nu_{\rm min}$	GeV	10	30	7	...	...	2	...	...	2	...
$\nu_{\rm max}$	GeV	85	170	23	...	...	24	...	...	9.5	...
$z_{\rm min}$		0.2	...	0.2	...	...	0.1	...	...	0.2	...
$z_{\rm max}$		1	...	1	...	...	1	...	...	1	...
$E_{h\rm min}$	GeV	3	3	1.4	2.5	4	0.6	2	4	1	2.5†
$E_{h\rm max}$	GeV	85	170	23	15	...	15	...	...	9.5	...

TABLE II: Kinematic cuts of the EMC and HERMES experiments. They are divided into DIS cuts (upper group) and semi-inclusive cuts (lower group). In order to highlight the differences, 3 dots are used in place of the value found at their left. Notes: † L.LaGamba, who performed a cross-check of the analysis in [19], privately told me that pions results are compatible with $E_{h\rm min} = 1$ and not 2.5 GeV.

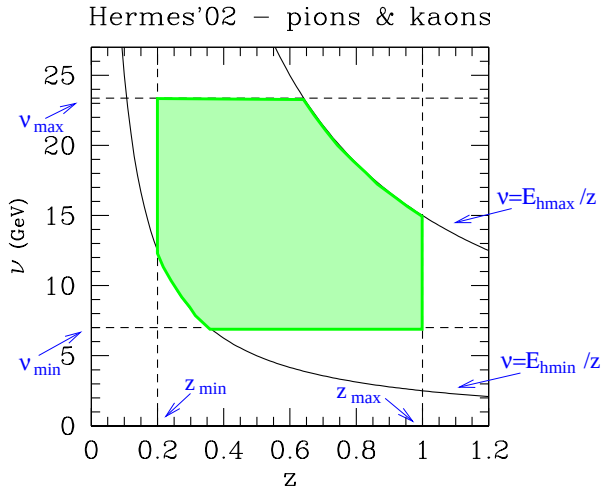

FIG. 7: Kinematic cuts for HERMES π and K production on N and Kr targets.